Cellular and Molecular Biology
E-ISSN : 1165-158X / P-ISSN : 0145-5680
www.cellmolbiol.org

# MiR-669b-5p inhibits the Alzheimer's disease development via regulation of CHEK2 in Neuro2a APPSwe/Δ9 cells

Mula A[1], Yan Bai[1], Bingcheng Hu[1], Yunhai Su[1], Xingxing Yuan[2*]

[1] Department of Encephalopathy, Heilongjiang Academy of Traditional Chinese Medicine, No. 33 of West Dazhi Street, Harbin, Heilongjiang 150001, P.R. China

[2] Department of General Medicine, Heilongjiang Academy of Traditional Chinese Medicine, No. 33 of West Dazhi Street, Harbin, Heilongjiang 150001, P.R. China

**ARTICLE INFO**

***Original paper***

***Article history:***
*Received: July 18, 2023*
*Accepted: September 15, 2023*
*Published: September 30, 2023*

***Keywords:***

*miR-669b-5p, CHEK2, Aβ; Alzheimer, Neuro2a APPSwe/Δ9 cells*

**ABSTRACT**

DNA damage of neurons is accumulated in Alzheimer's disease (AD). DNA damage-activated Checkpoint kinase 2 (CHEK2) is evaluated in Aβ-treated Neuro2a APPSwe/Δ9 cells, and the miR-669b-5p was specifically down-regulated. However, the underlying molecular mechanism between CHEK2 and miR-669b-5p in Neuro2a APPSwe/Δ9 cells remains unclear. This research discovers that in A-treated Neuro2a APPSwe/Δ9 cells, CHEK2 expression and miR-669b-5p expression were inversely correlated. In addition, miR-669b-5p mimics increased cell survival and proliferation in Neuro2a APPSwe/Δ9 cells while decreasing the production of inflammatory cytokines and cell death. Furthermore, it is observed that CHEK2 was a miR-669b-5p downstream target gene and that CHEK2 restored the miR-669b-5p's functions. According to this research, miR-669b-5p is a potential therapy for Alzheimer's patients since it slows the advancement of the disease.

**Doi:** http://dx.doi.org/10.14715/cmb/2023.69.9.17


## Introduction

The most well-known form of dementia in humans, Alzheimer's disease (AD), lacks an effective treatment (1, 2). The two primary characteristics of AD are neurofibrillary tangles and senile plaques (SPs), with β-amyloid (Aβ) peptide constituting the majority of SPs (3, 4). The Aβ peptide is cleaved from the amyloid precursor protein byγ-secretase complex and β-secretase (5, 6). But the underlying molecular regulation mechanism of Alzheimer's disease development needed further research.

It has been found that the DNA damage of neurons accumulated in normal aging and AD (7, 8). DNA damage-activated Checkpoint kinase 2 (CHEK2) is a Ser/Thr kinase and it enhances tau toxicity by phosphorylating tau in a transgenic Drosophila model (2, 8). CHEK2 influence the DNA damage response, including cell cycle checkpoint regulators, DNA repair, and apoptosis by phosphorylating related proteins (8). In this study, we found that CHEK2 was up-regulated in Aβ-treated Neuro2a APPSwe/Δ9 cells. It implied that CHEK2 was involved in the disease progression of AD.

MicroRNAs (miRNAs) are non-coding RNAs that are present in a variety of animals. They attach to the 3'-UTR of the target gene's mRNA to control the translation of the target gene. According to earlier research, miRNAs are possible biomarkers for several illnesses (9-11). Among them, several miRNAs express abnormally and contribute to neuronal dysfunction (6, 12, 13). For instance, miR-125b controls brain cell growth and death, contributing to AD onset (14). MiR-137 and CACNA1C gene expression in the transgenic mice model of AD prevents tau protein from being hyperphosphorylated (15). By inhibiting the expressions of TTBK1 as well as GSK-3β, miR-219-5p substantially alleviates AD-like symptoms in amyloid precursor protein/presenilin 1 mice (12). Long-lived mice's neuronal function is benefited from the up-regulation of miR-669b, which is implicated in the posttranscriptional control of genes relevant to growth hormone/IGF1 signaling (16). But the several studies mentioned the function of miR-669b and related miRNAs during the occurrence and development of AD diseases.

In our study, we predicted that miR-669b-5p was related to CHEK2 by bioinformatics in Neuro2a APPSwe/Δ9 cells. And then we investigated the pathological effect of miR-669b-5p in AD and the possible molecular mechanisms between miR-669b-5p and CHEK2. We found that miR-669b-5p mimics inhibited inflammation and cell apoptosis in Neuro2a APPSwe/Δ9 cells. Additionally, miR-669b-5p mimics were no longer inhibited when CHEK2 was overexpressed. All of the findings suggested that miR-669b-5p, a novel molecular regulatory mechanism in Alzheimer's disease, reduced inflammation and cell death by targeting CHEK2.

* Corresponding author. Email: jackie198711@163.com

## Materials and Methods

### Cell culture and treatment

Cells for Neuro2a APPSwe/Δ9 were provided by the Cell Bank of Type Culture Collection of the Chinese Academy of Sciences (Shanghai, China). Neuro2a APPSwe/Δ9 cells were cultivated in Opti-MEM with 5% fetal bovine serum in 5% $CO_2$ at 37°C and Dulbecco's modified Eagle's media (DMEM; 10569010, Gibco; Thermo Fisher Scientific, Inc.). 10μM Aβ (Abeta-42, 107761-42-2, Sigma, USA) was applied to cells for 24 h (17) before they were harvested and removed for testing.

### qRT-PCR assay

Utilizing TRIzol (Takara, D9108A, Japan) reagents, total RNA was extracted from the Neuro2a APPSwe/Δ9 c/ells that had undergone treatment. A 4800 real-time PCR system (Bio-Rad) was applied to conduct quantitative real-time PCR (qRT-PCR). Using Takara's RR036A SYBR® Green Master Mix, the reactions were conducted. 20 μL of SYBR Green PCR Master Mix (Invitrogen), 1 μL of each F or R primer, 4 μL of DEPC water, and 5 μL of cDNA were used for real-time PCR utilizing the $2^{-\Delta\Delta CT}$ technique. Following 94°C for 3 min, there were 35 cycles of 94°C for 10 s and 63°C for 30 s in the PCR operation. The primers for RT-qPCR were as followed: mmu-miR-669b-5p: 5′- ACACTCCAGCTGGGAGCTTATCAGACTGA-3′ (Forward) and 5′-TGGTGTCGTGGACTCC-3′ (Reverse); CHEK2: 5'-TCTCGGGAGTCGGATGTTGAG-3' (Forward) and 5'-CCTGAGTGGACACTGTCTCTAA-3' (Reverse); mmu-U6: 5′-CTCGCTTCGGCAGCACA-3′ (Forward) and 5′-AACGCTTCACGAATTTGCGT-3′ (Reverse); mmu-β-actin: 5′-CATGTACGTTGCTATCCAGGC-3' (Forward) and 5′-CTCCTTAATGTCACGCACGAT-3′ (Reverse).

### Western blotting

A polyvinylidene fluoride membrane (Millipore, Billerica, MA, USA) was used to transfer the protein samples after 10% SDS-PAGE separation. Primary antibodies included those against Bax (ab32503), Bcl-2 (ab32124), cleaved Caspase-3 (ab32042), cleaved Caspase-9 (ab2324), anti-β-actin (ab8226), and CHEK2 (ab109413, Abcam, Cambridge, UK). With the use of Millipore's ECL detection reagent, immunoreactive bands were seen. ImageQuant 1D software (GE Healthcare, Pittsburgh, PA, United States) measured the density of the bands. β-actin served as the internal control.

### ELISA Assay

At 37°C, in 5% $CO_2$ with 95% air, 100 microliters of cells ($2\times10^6$/mL), 20 microliters of the medium, and 80 μL of cultivated supernatant were combined. The cells were centrifuged after incubation, and the culture supernatants were obtained. Then, using widely available human cytokine ELISA kits, the concentration of several cytokines in cell-free culture supernatants was determined (17). Applying an enzyme-linked immunosorbent assay (ELISA) kit from R&D in the USA, the supernatants of cells were collected and tested for the presence of IL-1β, TNF-α, IL-6, as well as IL-10. 50 μL of the samples were utilized for each experiment, which employed duplicate samples and expressed the cytokines' levels in pg/mg. Every experiment included the running of standards, and standard curves was produced for each test. The Bio-Plex Manager program was used to calculate sample concentrations.

### CCK-8 Assay

To identify cell proliferation, CCK-8 Assay Cell Counting Kit-8 (CCK-8) (Sigma, USA) was utilized. MiR-669b-5p and NC mimics were transfected into cells by Lipo3000 following the manufacturer's instructions. Thermo Fisher Scientific, Inc.'s UV spectrophotometer was utilized to detect the OD value at 450 nm.

### TUNEL assay

The TUNEL test was also applied to identify cell apoptosis. And the experiment was performed using a commercial Cell Death Detection kit (Roche Molecular Diagnostics) following the kit's instructions. Cells were fixed in 4% paraformaldehyde for 15 min, permeabilized with 0.25% Triton-X 100, and then the assay was performed. A scanning microscope was used to count the TUNEL-positive cells at a magnification of ×400.

### Flow cytometry assay

Apoptotic cells were identified using the flow cytometry test FITC-Annexin V/PI apoptotic detection kit (BD ingen, San Diego, CA, USA). Propidium iodide (4.5 mL), as well as Annexin V-FITC (4.5 mL), were used to stain the cells ($1\times10^5$ cells), followed by fluorescence detection using a flow cytometer (Beckman, Miami, FL, USA).

### Luciferase reporter assay

According to the sequence of miR-669b-5p, WT or mutant (MUT) CHEK2 3'-UTR sequences were chemically produced (Sangon, Shanghai, China). According to the instructions provided with the kit (Promega, USA), the luciferase activity was discovered by the luciferase reporter assay method.

### EdU assay

In terms of a prior description (18), the EdU test (Solarbio, Beijing, China) was used to measure cell proliferation. 24-well plates containing Neuro2a APPSwe/Δ9 cells ($2\times10^4$ cells/well) were planted, and the cells were then treated in DMEM containing 10% FBS for 24 h. Each well had EdU added for two hours. The cells were stained with 1×Apollo for 30 min in the dark after fixation. The nucleus was then stained for 5 min using DAPI. The fluorescent microscope (Olympus, Tokyo, Japan) was applied to identify cells.

### Statistical analysis

The standard±deviation (SD) is employed to show data. Unpaired/paired Student's t-test, Mann-Whitney test, one-way ANOVA, and Bonferroni's post hoc test were applied to evaluate comparisons. At $P<0.05$, the differences were declared statistically significant.

## Results

### The expression of CHEK2 is up-regulated in Aβ-treated Neuro2a APPSwe/Δ9 cells

Neuro2a APPSwe/Δ9 cells were processed with 0μM or 10μM Aβ. The expression of CHEK2 was evaluated in Aβ-treated Neuro2a APPSwe/Δ9 cells by qRT-PCR (Figure 1A), and Aβ increased the protein level of CHEK2

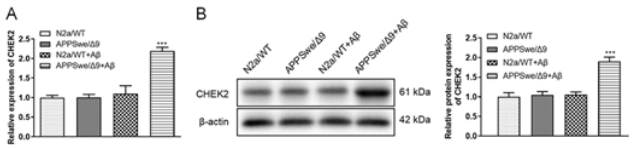


**Figure 1.** The expression of CHEK2 was detected in Aβ-treated Neuro2a APPSwe/Δ9 cells. Neuro2a APPSwe/Δ9 cells were treated with 10 μM Aβ for 24 h. (A) qRT-PCR tested the expression of CHEK2 in Aβ-treated Neuro2a APPSwe/Δ9 cells. (B) Western blot analysis of the expression levels of CHEK2 in Aβ-treated Neuro2a APPSwe/Δ9 cells. Values are mean ± SD, ***P<0.001 vs. APPSwe/Δ9 group. n=3 per group.

in Neuro2a APPSwe/Δ9 cells by western blot (Figure 1B). These results confirmed that CHEK2 was up-regulated in Aβ-treated Neuro2a APPSwe/Δ9 cells.

**CHEK2 is a downstream target of miR-669b-5p.**

CHEK2 has been proven to be involved in tau phosphorylation and toxicity in the pathogenesis of AD (8). To explore the regulatory mechanism of CHEK2 in Aβ-treated Neuro2a APPSwe/Δ9 cells, we used miRwalk and miRDB to search the related miRNAs and finally found 5 intersection miRNAs (Figure 2A). The qRT-PCR outcomes illustrated that miR-669b-5p was specifically downregulated in Aβ-treated Neuro2a APPSwe/Δ9 cells (Figure 2A). The probable interaction site between CHEK2 and miR-669b-5p was then predicted using StarBase (Figure 2B). Next, we used luciferase reporter research to discover how CHEK2 and miR-669b-5p interact. The findings demonstrated that co-transfection of CHEK2-WT and miR-669b-5p mimics dramatically decreased the luciferase activity of CHEK2's 3'UTR region in Neuro2a APPSwe/Δ9 cells. However, there was no discernible difference between the miR-669b-5p mimics group as well as CHEK2-Mut in terms of luciferase activity (Figure 2C).

At the levels of both mRNA and protein, miR-669b-5p mimics consistently reduce CHEK2 expression in Neuro2a APPSwe/Δ9 cells (Figure 2D-E). According to the results of Figure 1A, there are two other miRNAs which are significantly upregulated: miR-12205-5p and miR-7021-3p. In order to eliminate the interference of these two miRNAs, we detected the expression level of CHEK2 (Figure 2F) after over-expression. The results showed that miR-12205-5p and miR-7021-3p could not specifically reduce the expression of CHEK2, which indicated that the regulation of CHEK2 by miR-665b-5p was specific. In addition, the addition of anti-miR-669-5p can specifically reduce the expression of CHEK2 (Figure 2G). In general, in terms of these data, CHEK2 was a downstream target gene of miR-669b-5p, and CHEK2 was inversely linked with miR-669b-5p.

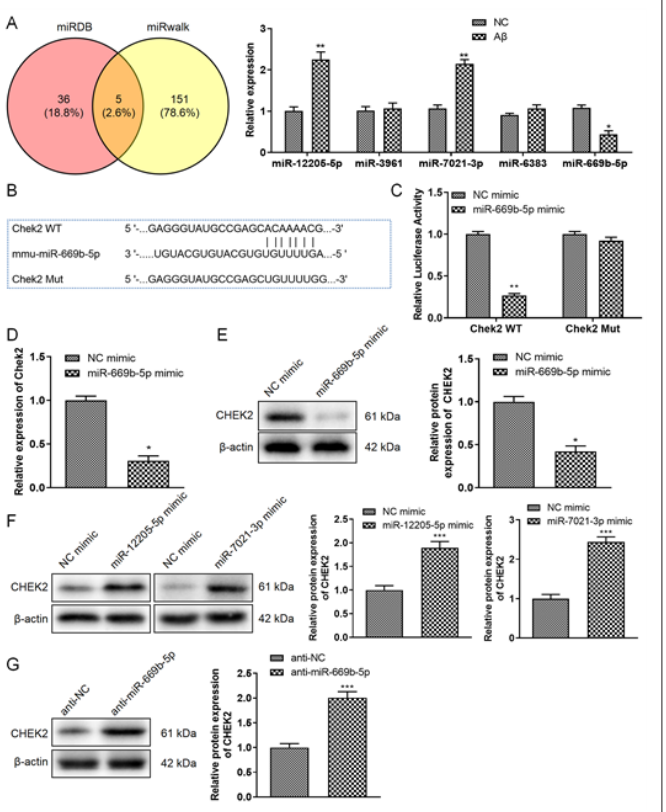


**Figure 2.** CHEK2 is a downstream target of miR-669b-5p. (A) We used miRwalk and miRDB to search the related target genes. Then qRT-PCR tested the expression of 5 intersection target genes in Aβ-treated Neuro2a APPSwe/Δ9 cells. Values were mean ± SD, *P<0.05 and **P<0.01 vs. NC group. n=3 per group. (B) Bioinformatic analysis of the predicted binding sites of CHEK2 and miR-669b-5p. (C) Luciferase reporter assay was performed after 48 h transfection in Neuro2a APPSwe/Δ9 cells with a luciferase reporter plasmid containing WT or mutant form of CHEK2 3′-UTR along with NC mimics or miR-669b-5p mimics. (D) NC mimics or miR-669b-5p mimics were transfected in Neuro2a APPSwe/Δ9 cells, and the expression of CHEK2 was analyzed by qRT-PCR. (E-G) The protein level of CHEK2 was detected by western blot. Values were mean ± SD, *P<0.05, **P<0.01 and ***P<0.001 vs. NC mimics or anti-NC group. n=3 per group.

**MiR-669b-5p mimics promote proliferation and inhibit apoptosis of Neuro2a APPSwe/Δ9 cells.**

To further understand the biological role of miR-669b-5p in Neuro2a APPSwe/Δ9 cells, miR-669b-5p mimics and NC mimics were transfected into the cells, respectively.

In comparison to the NC mimic group, miR669b-5p mimics elevated miR669b-5p, according to qRT-PCR data (Figure 3A). Functionally, the CCK-8 and EdU experiments demonstrated that miR-669b-5p mimics improved the viability and proliferation of Neuro2a APPSwe/Δ9 cells (Figure 3B-C). The expression of proteins linked to proliferation was then analyzed by western blot. Expression levels of proliferation-related antigen (Ki-67) and proliferating cell nuclear antigen (PCNA) were discovered to be greater in the miR-669b-5p mimics group (Figure 3D). The overexpression of miR-669b-5p decreased cell death in Neuro2a APPSwe/Δ9 cells, as revealed by the flow cytometry experiment (Figure 3E). Furthermore, to examine the expression of proteins related to apoptosis, a western blot was performed. We noticed that mimics of miR-669b-5p increased the production of pro-apoptotic proteins (Bax, Cleaved caspase-3, and Cleaved caspase-9) while suppressing the expression of the anti-apoptotic protein (Bcl-2) (Figure 3F). The overexpression of miR-669b-5p in Neuro2a APPSwe/Δ9 cells led to the proliferation and prevented apoptosis, according to all the data.

**Overexpression of miR-669b-5p inhibits the expression of inflammatory cytokines**

MiR-669b-5p mimics and NC mimics were transfected into Neuro2a APPSwe/Δ9 cells. MiR-669b-5p mimics

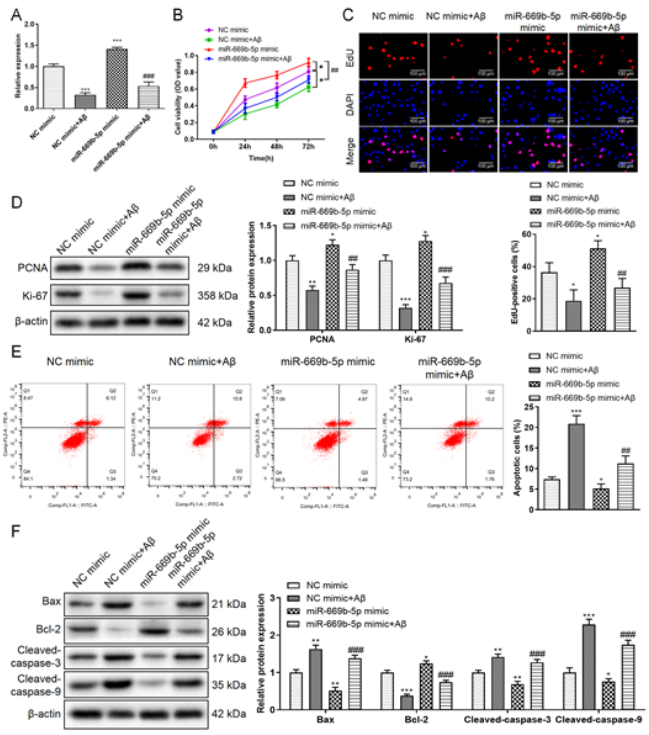


**Figure 3.** MiR-669b-5p mimics promote proliferation and inhibit apoptosis of Neuro2a APPSwe/Δ9 cells. MiR-669b-5p mimics and NC mimics were transfected in Neuro2a APPSwe/Δ9 cells. (A) The expression of miR-669b-5p was analyzed by qRT-PCR. (B) The cell viability of Neuro2a APPSwe/Δ9 cells was detected by CCK-8 assay. (C) EdU assay to analyze the cell proliferation of Neuro2a APPSwe/Δ9 cells. (D) The protein level of PCNA and Ki-67 was tested by western blot. (E-F) The apoptosis of Neuro2a APPSwe/Δ9 cells was detected by FCM and TUNEL. (G) The protein level of apoptosis-associated proteins (Bax, Bcl-2, Cleaved caspase-3, and Cleaved caspase-9) were detected by western blot. Values are mean ± SD, *P<0.05, **P<0.01 and ***P<0.001 vs. NC mimics group, ##P<0.01 and ###P<0.001 vs. miR-669b-5p mimics group. n=3 per group.

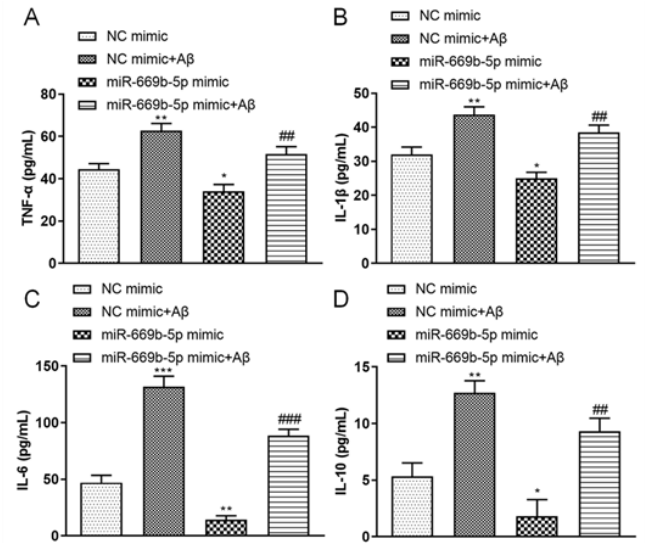


**Figure 4.** Overexpression of miR-669b-5p inhibits the expression of inflammatory cytokines. MiR-669b-5p mimics and NC mimics were transfected in Neuro2a APPSwe/Δ9 cells. (A-D) The cytokine release of TNF-α, IL-1β, IL-6 and IL-10 was detected by ELISA. Values were mean ± SD, *P<0.05, **P<0.01 and ***P<0.001 vs. NC mimics group, ##P<0.01 and ###P<0.001 vs. miR-669b-5p mimics group. n=3 per group.

reduced the release of inflammatory cytokines, including TNF-α, IL-1β, IL-6, and IL-10 (Figure 4A-D). Additionally, miR-669b-5p mimics enhanced the production of the anti-inflammatory cytokine IL-10. This finding demonstrated that miR-669b-5p mimics limit inflammatory cytokine expression while promoting anti-inflammatory cytokine expression.

**Overexpression of miR-669b-5p reduces oxidative stress**

To find out the biological role of miR-669b-5p in oxidative stress, miR-669b-5p mimics and NC mimics were transfected into Neuro2a APPSwe/Δ9 cells. The DCFH-DA assay was applied to measure the levels of oxidative stress in Neuro2a APPSwe/Δ9 cells transfected with miR-669b-5p mimics. The mean fluorescence intensity (MFI) of intracellular ROS was decreased (Figure 5A). Furthermore, the SOD enzyme activity was markedly elevated by miR-669b-5p mimics, whereas the MDA content was reduced in comparison with control cells (Figure 5B-C). All the results showed that miR-669b-5p mimics reduced oxidative stress in Neuro2a APPSwe/Δ9 cells.

**MiR-669b-5p mimics inhibit the expression of APP, BACE1, phosphorylation Tau1, and Aβ.**

A western blot assay was conducted to test the expressions of APP, BACE1, phosphorylation Tau1 (p-Tau1), and amyloid-beta (Aβ), and found that the miR-669b-5p mimics downregulated the expression of APP, BACE1, p-Tau1 and Aβ (Figure 6A-B). Meanwhile, the Aβ release of Neuro2a APPSwe/Δ9 cells was inhibited by miR-669b-5p mimics via ELISA assay (Figure 6C). These indicated that miR-669b-5p mimics played a protective role in Neuro2a APPSwe/Δ9 cells by downregulating the expression of APP, BACE1, p-Tau1, and Aβ.

**Rescue experiments verify that miR-669-5p/CHEK2 regulates the occurrence and development of Alzheimer's disease**

The rescue experiment was the next step in our investigation into the role of miR-669-5p/CHEK2 in Neuro2a

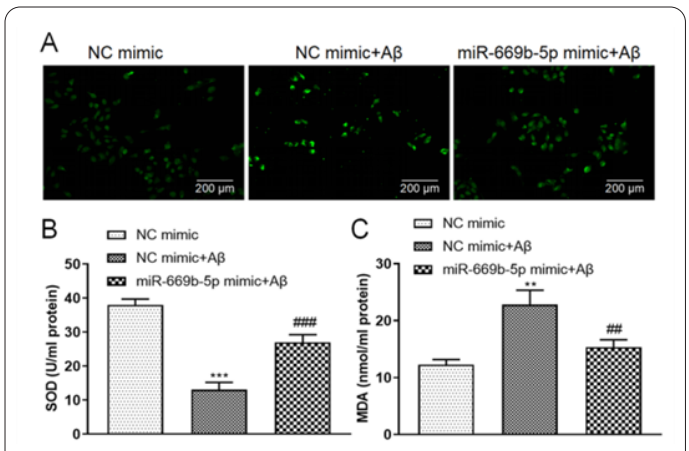


**Figure 5.** Overexpression of miR-669b-5p reduces oxidative stress. MiR-669b-5p mimics and NC mimics were transfected in Neuro2a APPS we/Δ9 cells. (A) The ROS level of Neuro2a APPSwe/Δ9 cells was tested by DCFH-DA assay. (B) The SOD enzyme activity was detected by the SOD kit. (C) MDA levels of these samples were measured at 532 nm using the MDA kit. Values were mean ± SD, *P<0.05, **P<0.01 and ***P<0.001 vs. NC mimics group, ##P<0.01 and ###P<0.001 vs. NC mimics+Aβ group. n=3 per group.

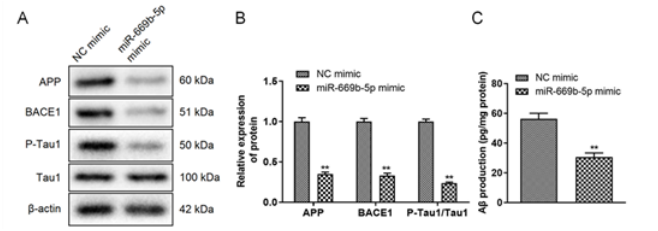


**Figure 6.** MiR-669b-5p mimics inhibit the expression of APP, BACE1, phosphorylation Tau1, and Aβ. MiR-669b-5p mimics and NC mimics were transfected in Neuro2a APPSwe/Δ9 cells. (A) The protein expression level of APP, BACE1, p-Tau1, and Aβ was detected by western blot. (B) The mRNA level of APP, BACE1, p-Tau1, and Aβ were analyzed by qRT-PCR. (C) The release of Aβ was detected by ELISA. Values were mean ± SD, **P<0.01 vs. NC mimics. n=3 per group.

APPSwe/Δ9 cells. First, qRT-PCR analysis demonstrated that miR-669b-5p mimics increased the expression of miR-669-5p. Additionally, according to a western blot analysis of Neuro2a APPSwe/Δ9 cells transfected with pc-CHEK2, CHEK2 expression was increased as compared with the pc-NC group (Figure 7A). The promoting impact of miR-669b-5p mimics was then found to be abolished by up-regulating CHEK2 in Neuro2a APPSwe/Δ9 cells by CCK-8 and EdU tests (Figure 7B-C, Figure S1A). Additionally, to examine the expression of proteins related to proliferation, a western blot was employed. The findings demonstrated that miR-669b-5p mimics raised PCNA and Ki-67 protein levels whereas pc-CHEK2 partially suppressed PCNA and Ki-67 expression as determined by miR-669b-5p mimics (Figure 7D, Figure S1B). The flow cytometry assay elucidated that pc-CHEK2 partly reversed the cell apoptosis inhibited by miR-669b-5p mimics in Neuro2a APPSwe/Δ9 cells (Figure 7E, Figure S1C). Also, the quantity of TUNEL-positive cells tested in Neuro2a APPSwe/Δ9 cells was partly increased by pc-CHEK2 compared to the miR-669b-5p mimics group (Figure 7F, Figure S1D).

In addition, we found that the increasing levels of anti-apoptosis proteins Bcl-2 and the decline of pro-apoptosis proteins (Bax, Cleaved caspase-3 as well as Cleaved caspase-9) were reserved by pc-CHEK2 partly via western blot analysis (Figure 7G, Figure S1E). The release of inflammatory cytokines TNF-α, IL-1β as well as IL-6 was partly increased by pc-CHEK2 compared to the miR-669b-5p mimics group (Figure 7H). While the anti-inflammatory cytokine IL-10 was partly declined by pc-CHEK2 compared to the miR-669b-5p mimics group (Figure 7H). The mean fluorescence intensity (MFI) of intracellular ROS declined by miR-669b-5p mimics and was partly reserved by pc-CHEK2 (Figure 7I). In the meanwhile, the enzyme activities of SOD elevated by miR-669b-5p mimics were partly reserved by pc-CHEK2, and the MDA content reduced by miR-669b-5p mimics was partly reserved by pc-CHEK2 (Figure 7I). Western blot assay displayed that the up-regulated expression of APP, BACE1, p-Tau1, and Aβ by miR-669b-5p mimics was partly reserved by pc-CHEK2 (Figure 7J, Figure S1F). Finally, pc-CHEK2 reserved the inhibition of Aβ released by miR-669b-5p mimics via ELISA assay (Figure 7K). In general, those results indicated that miR-669b-5p inhibited the development of Alzheimer's disease, and overexpression of CHEK2 rescued the effect of miR-669b-5p in Neuro2a

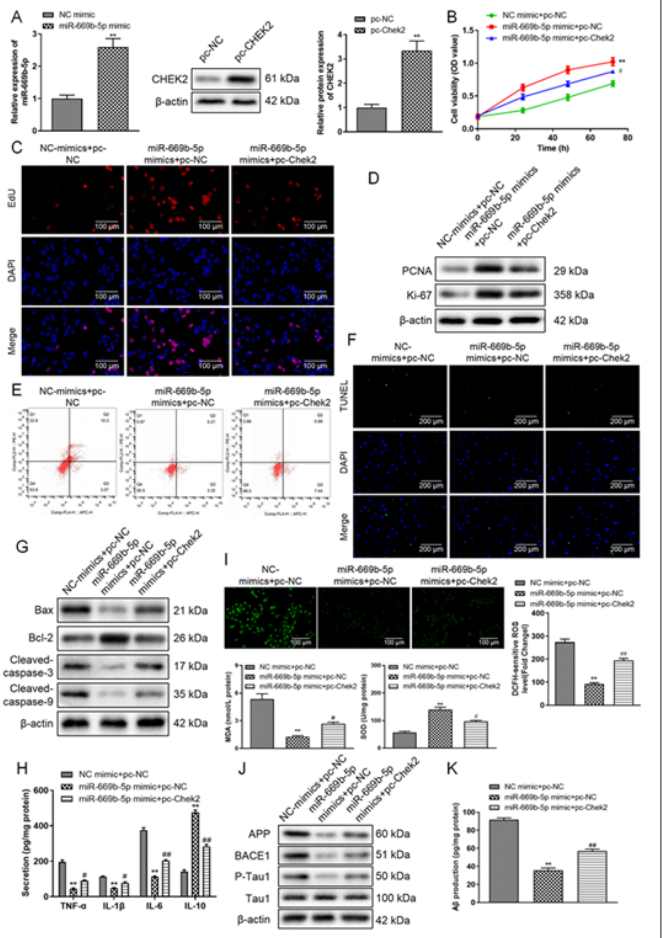


**Figure 7.** Rescue experiments verify that miR-669-5p/CHEK2 regulates the occurrence and development of Alzheimer's disease. (A) MiR-669b-5p mimics or pc-CHEK2 were transfected in Neuro2a APPSwe/Δ9 cells. The expression of miR-669-5p was tested by qRT-PCR. And the expression of CHEK2 was detected by western blot. Values are mean ± SD, **P<0.01 vs. NC mimics or pc-NC. n=3 per group. MiR-669b-5p mimics and pc-CHEK2 were co-transfected in Neuro2a APPSwe/Δ9 cells. (B) Cell viability was analyzed by CCK-8. (C) EdU assay to analyze cell proliferation. (D) The protein level of PCNA and Ki-67 was detected by western blot. (E) The apoptosis was detected by FCM. (F) The apoptosis of cells was detected by TUNEL assay. (G) The protein level of Bax, Bcl-2, Cleaved caspase-3, and Cleaved caspase-9 was detected by western blot. (H) The cytokines release of TNF-α, IL-1β, IL-6, and IL-10 was detected by ELISA (I) The ROS level was tested by DCFH-DA assay. The SOD enzyme activity was detected by the SOD kit. MDA level was measured by MDA kit. (J) The protein level of Bax, Bcl-2, Cleaved caspase-3, and Cleaved caspase-9 was tested by western blot. (K) ELISA was used to detect the release of Aβ. Values were mean ± SD, **P<0.01 vs. NC mimics+pc-NC group, #P<0.05 and ##P<0.01 vs. miR-669b-5p mimics+pc-NC group. n=3 per group.

APPSwe/Δ9 cells.

## Discussion

Around the world, AD is becoming increasingly prevalent, and it is predicted that by 2050, more than 35 million individuals would be affected (15). Although a great deal of study has been devoted to understanding the pathophysiology of AD and how to avoid it (19, 20), little is still known about these mechanisms.

CHEK2 plays regulatory roles in DNA repair and cell

cycle progression by phosphorylating downstream effectors (1). According to a publication, CHEK2 phosphorylates tau at Ser262 in the microtubule-binding domain, which is connected to AD (8). Furthermore, it has been proposed that tau hyperphosphorylation promotes the etiology of Alzheimer's disease (AD) in AD brains (12, 21). All of these findings suggested that CHEK2 controlled tau's aberrant phosphorylation and took a role in the onset of AD illness. In this investigation, we discovered that the expression of CHEK2 was inversely linked with the expression of miR-669b-5p in Neuro2a APPSwe/Δ9 cells and that CHEK2 was increased in Aβ-treated Neuro2a APPSwe/Δ9 cells. These findings indicated that a molecular control pathway exists between miR-669b-5p and CHEK2 in Neuro2a APPSwe/Δ9.

There are lots of studies finding showed that miRNAs regulated critical proteins and key biological processes in the progression and pathophysiology of AD (22), such as levels of Aβ, cell viability, cell apoptosis, and inflammation (23-25). For example, the inhibitor of miR-128 upregulated the expression of PPAR-γ to reduce Aβ-mediated cytotoxicity via inactivation of NF-κB in N2a cells (26). Others have shown that miR-124 encourages mouse neuroblastoma N2a cells to differentiate toward a neuronal phenotype (27-29). In this work, we hypothesized that miR-669b-5p was associated with CHEK2 in Neuro2a APPSwe/Δ9 cells using bioinformatics. The function and effect of miR-669b-5p in the onset and progression of AD illness, however, has received less attention in the literature. Then, using luciferase reporter research, we discovered that CHEK2 was a miR-669b-5p's fundamental target. Functional analysis of Neuro2a APPSwe/Δ9 cells revealed that overexpression of miR-669b-5p increased cell proliferation while inhibiting cell death, oxidative stress, and inflammatory cytokine production.

At the end of this study, we performed rescue experiments to further explore the regulation mechanism between miR-669b-5p and CHEK2. It was confirmed that the CHEK2 overexpression party reversed the protection of the overexpression of miR-669b-5p in Neuro2a APPSwe/Δ9 cells.

In conclusion, all findings demonstrated that overexpression of miR-669b-5p protected Neuro2a APPSwe/Δ9 cells by promoting the viability of cells, inhibiting cell apoptosis, oxidative stress, and secretion of inflammation-related cytokines. MiR-669b-5p exerted protective functions by targeting CHEK2. Our study demonstrated the regulation mechanism and function between miR-669b-5p and CHEK2 in Neuro2a APPSwe/Δ9 cells *in vitro*. And the molecular regulation and function of miR-669b-5p and CHEK2 needed to be confirmed *in vivo* in the future. Furthermore, this study provided a novel and promising therapeutic target for AD.

**Acknowledgments**
We thank the Heilongjiang Province TCM Research Project for funding.

**Interest conflict**
The authors promise to have no conflicts of interest.

**Consent for publications**
The author read and proved the final manuscript for publication.

**Availability of data and material**
All data generated during this study are included in this published article

**Authors' Contribution**
All authors had equal roles in study design, work, statistical analysis, and manuscript writing.

**Funding**
This work was supported by the Traditional Chinese Medicine Research Project of Heilongjiang Province (ZHY2022-080).

**Ethics approval and consent to participate**
No humans or animals were used in the present research.

**References**

1. Mendoza J, Sekiya M, Taniguchi T, Iijima KM, Wang R, and Ando K. Global analysis of phosphorylation of tau by the checkpoint kinases Chk1 and Chk2 in vitro. J Proteome Res. 2013;12(6):2654-65. doi: 10.1021/pr400008f.
2. Iijima K, Gatt A, and Iijima-Ando K. Tau Ser262 phosphorylation is critical for Abeta42-induced tau toxicity in a transgenic Drosophila model of Alzheimer's disease. Hum Mol Genet. 2010;19(15):2947-57. doi: 10.1093/hmg/ddq200.
3. Roher AE, Kokjohn TA, Clarke SG, Sierks MR, Maarouf CL, Serrano GE, et al. APP/Abeta structural diversity and Alzheimer's disease pathogenesis. Neurochem Int. 2017;110:1-13. doi: 10.1016/j.neuint.2017.08.007.
4. Dunys J, Valverde A, and Checler F. Are N- and C-terminally truncated Abeta species key pathological triggers in Alzheimer's disease? J Biol Chem. 2018;293(40):15419-15428. doi: 10.1074/jbc.R118.003999.
5. Zhang X, Wang J, Gong G, Ma R, Xu F, Yan T, et al. Spinosin Inhibits Abeta(1-42) Production and Aggregation via Activating Nrf2/HO-1 Pathway. Biomol Ther (Seoul). 2020;28(3):259-266. doi: 10.4062/biomolther.2019.123.
6. Salta E, Sierksma A, Vanden Eynden E, and De Strooper B. miR-132 loss de-represses ITPKB and aggravates amyloid and TAU pathology in Alzheimer's brain. EMBO Mol Med. 2016;8(9):1005-18. doi: 10.15252/emmm.201606520.
7. Moreira PI, Nunomura A, Nakamura M, Takeda A, Shenk JC, Aliev G, et al. Nucleic acid oxidation in Alzheimer disease. Free Radic Biol Med. 2008;44(8):1493-505. doi: 10.1016/j.freeradbiomed.2008.01.002.
8. Iijima-Ando K, Zhao L, Gatt A, Shenton C, and Iijima K. A DNA damage-activated checkpoint kinase phosphorylates tau and enhances tau-induced neurodegeneration. Hum Mol Genet. 2010;19(10):1930-8. doi: 10.1093/hmg/ddq068.
9. Wu Y, Xu J, Xu J, Cheng J, Jiao D, Zhou C, et al. Lower Serum Levels of miR-29c-3p and miR-19b-3p as Biomarkers for Alzheimer's Disease. Tohoku J Exp Med. 2017;242(2):129-136. doi: 10.1620/tjem.242.129.
10. Wang X, Liu D, Huang HZ, Wang ZH, Hou TY, Yang X, et al. A Novel MicroRNA-124/PTPN1 Signal Pathway Mediates Synaptic and Memory Deficits in Alzheimer's Disease. Biol Psychiatry. 2018;83(5):395-405. doi: 10.1016/j.biopsych.2017.07.023.
11. Switlik W, Karbownik MS, Suwalski M, Kozak J, and Szemraj J. miR-30a-5p together with miR-210-3p as a promising biomarker for non-small cell lung cancer: A preliminary study. Cancer Biomark. 2018;21(2):479-488. doi: 10.3233/CBM-170767.
12. Li J, Chen W, Yi Y, and Tong Q. miR-219-5p inhibits tau phosphorylation by targeting TTBK1 and GSK-3beta in Alzheimer's

disease. J Cell Biochem. 2019;120(6):9936-9946. doi: 10.1002/jcb.28276.

13. Ji Y, Wang D, Zhang B, and Lu H. MiR-361-3p inhibits beta-amyloid accumulation and attenuates cognitive deficits through targeting BACE1 in Alzheimer's disease. J Integr Neurosci. 2019;18(3):285-291. doi: 10.31083/j.jin.2019.03.1136.
14. Jin Y, Tu Q, and Liu M. MicroRNA-125b regulates Alzheimer's disease through SphK1 regulation. Mol Med Rep. 2018;18(2):2373-2380. doi: 10.3892/mmr.2018.9156.
15. Jiang Y, Xu B, Chen J, Sui Y, Ren L, Li J, et al. Micro-RNA-137 Inhibits Tau Hyperphosphorylation in Alzheimer's Disease and Targets the CACNA1C Gene in Transgenic Mice and Human Neuroblastoma SH-SY5Y Cells. Med Sci Monit. 2018;24:5635-5644. doi: 10.12659/MSM.908765.
16. Liang R, Khanna A, Muthusamy S, Li N, Sarojini H, Kopchick JJ, et al. Post-transcriptional regulation of IGF1R by key microRNAs in long-lived mutant mice. Aging Cell. 2011;10(6):1080-8. doi: 10.1111/j.1474-9726.2011.00751.x.
17. Gopalsamy B, Farouk AAO, Tengku Mohamad TAS, Sulaiman MR, and Perimal EK. Antiallodynic and antihyperalgesic activities of zerumbone via the suppression of IL-1beta, IL-6, and TNF-alpha in a mouse model of neuropathic pain. J Pain Res. 2017;10:2605-2619. doi: 10.2147/JPR.S143024.
18. Huang Y, Huang H, Wang S, Chen F, and Zheng G. Dehydrocorydaline inhibits the tumorigenesis of breast cancer MDA-MB-231 cells. Mol Med Rep. 2020;22(1):43-50. doi: 10.3892/mmr.2020.11122.
19. Li L, Sengupta A, Haque N, Grundke-Iqbal I, and Iqbal K. Memantine inhibits and reverses the Alzheimer type abnormal hyperphosphorylation of tau and associated neurodegeneration. FEBS Lett. 2004;566(1-3):261-9. doi: 10.1016/j.febslet.2004.04.047.
20. Reddy PH and McWeeney S. Mapping cellular transcriptosomes in autopsied Alzheimer's disease subjects and relevant animal models. Neurobiol Aging. 2006;27(8):1060-77. doi: 10.1016/j.neurobiolaging.2005.04.014.
21. Hanger DP, Byers HL, Wray S, Leung KY, Saxton MJ, Seereeram A, et al. Novel phosphorylation sites in tau from Alzheimer brain support a role for casein kinase 1 in disease pathogenesis. J Biol Chem. 2007;282(32):23645-54. doi: 10.1074/jbc.M703269200.
22. Reddy PH, Tonk S, Kumar S, Vijayan M, Kandimalla R, Kuruva CS, et al. A critical evaluation of neuroprotective and neurodegenerative MicroRNAs in Alzheimer's disease. Biochem Biophys Res Commun. 2017;483(4):1156-1165. doi: 10.1016/j.bbrc.2016.08.067.
23. Motti D, Bixby JL, and Lemmon VP. MicroRNAs and neuronal development. Semin Fetal Neonatal Med. 2012;17(6):347-52. doi: 10.1016/j.siny.2012.07.008.
24. Olsen LC, O'Reilly KC, Liabakk NB, Witter MP, and Saetrom P. MicroRNAs contribute to postnatal development of laminar differences and neuronal subtypes in the rat medial entorhinal cortex. Brain Struct Funct. 2017;222(7):3107-3126. doi: 10.1007/s00429-017-1389-z.
25. Xiao X, Jiang Y, Liang W, Wang Y, Cao S, Yan H, et al. miR-212-5p attenuates ferroptotic neuronal death after traumatic brain injury by targeting Ptgs2. Mol Brain. 2019;12(1):78. doi: 10.1186/s13041-019-0501-0.
26. Geng L, Zhang T, Liu W, and Chen Y. Inhibition of miR-128 Abates Abeta-Mediated Cytotoxicity by Targeting PPAR-gamma via NF-kappaB Inactivation in Primary Mouse Cortical Neurons and Neuro2a Cells. Yonsei Med J. 2018;59(9):1096-1106. doi: 10.3349/ymj.2018.59.9.1096.
27. Azizi Dargahlou, S., Iriti, M., Pouresmaeil, M., Goh, L. P. W. MicroRNAs; their therapeutic and biomarker properties. Cell Mol Biomed Rep 2023; 3(2): 73-88. doi: 10.55705/cmbr.2022.365396.1085
28. Kanwal, N., Al Samarrai, O., Al-Zaidi, H. M. H., Mirzaei, A., Heidari, M. Comprehensive analysis of microRNA (miRNA) in cancer cells. Cell Mol Biomed Rep 2023; 3(2): 89-97. doi: 10.55705/cmbr.2022.364591.1070.
29. You Q, Gong Q, Han YQ, Pi R, Du YJ, and Dong SZ. Role of miR-124 in the regulation of retinoic acid-induced Neuro-2A cell differentiation. Neural Regen Res. 2020;15(6):1133-1139. doi: 10.4103/1673-5374.270417.